ENVIRONMENTAL RESEARCH
LETTERS

LETTER • OPEN ACCESS

Increasing freshwater and dissolved organic carbon flows to Northwest Alaska's Elson lagoon

IOP Publishing Environ. Res. Lett. 16 (2021) 105014 https://doi.org/10.1088/1748-9326/ac2288

ENVIRONMENTAL RESEARCH
LETTERS

OPEN ACCESS

RECEIVED
20 May 2021

REVISED
4 August 2021

ACCEPTED FOR PUBLICATION
31 August 2021

PUBLISHED
12 October 2021

LETTER

Increasing freshwater and dissolved organic carbon flows to Northwest Alaska's Elson lagoon

Michael A Rawlins

Climate System Research Center, Department of Geosciences, University of Massachusetts, Amherst, MA, United States of America

E-mail: mrawlins@umass.edu

Keywords: dissolved organic carbon, permafrost, Arctic, freshwater export, northwest Alaska, climate change

Supplementary material for this article is available online

Abstract

Manifestations of climate change in the Arctic are numerous and include hydrological cycle intensification and permafrost thaw, both expected as a result of atmospheric and surface warming. Across the terrestrial Arctic dissolved organic carbon (DOC) entrained in arctic rivers may be providing a carbon subsidy to coastal food webs. Yet, data from field sampling is too often of limited duration to confidently ascertain impacts of climate change on freshwater and DOC flows to coastal waters. This study applies numerical modeling to investigate trends in freshwater and DOC exports from land to Elson Lagoon in Northwest Alaska over the period 1981–2020. While the modeling approach has limitations, the results point to significant increases in freshwater and DOC exports to the lagoon over the past four decades. The model simulation reveals significant increases in surface, subsurface (suprapermafrost), and total freshwater exports. Significant increases are also noted in surface and subsurface DOC production and export, influenced by warming soils and associated active-layer thickening. The largest changes in subsurface components are noted in September, which has experienced a ∼50% increase in DOC export emanating from suprapermafrost flow. Direct coastal suprapermafrost freshwater and DOC exports in late summer more than doubled between the first and last five years of the simulation period, with a large anomaly in September 2019 representing a more than fourfold increase over September direct coastal export during the early 1980s. These trends highlight the need for dedicated measurement programs that will enable improved understanding of climate change impacts on coastal zone processes in this data sparse region of Northwest Alaska.

1. Introduction

Arctic amplification is one of many hallmarks of earth's changing climate (Serreze *et al* 2009). Amplified rates of change across high northern latitudes (Holland and Bitz 2003, Box *et al* 2019) present challenges for establishing a fundamental understanding of Arctic coastal systems. Research efforts are further hindered by a paucity of long-term datasets that would facilitate differentiating new from normal baseline conditions. Field studies near Utqiaġvik (formerly Barrow), AK are providing baseline estimates of freshwater and nutrient flows to adjacent coastal waters (Lougheed *et al* 2020). Yet, such focused studies, while providing important data for understanding coastal zone structure and function and, in turn, its ecosystem services, are limited in their utility for assessing how terrestrial exports of freshwater and nutrients are changing under the influences related to climate warming. Coastal waters in northern Alaska receive freshwater from rivers rich in organic matter (McClelland *et al* 2014), with much of the influx occurring during the spring freshet that follows snowmelt. This flux of water-borne nutrients including dissolved organic carbon (DOC) strongly influences coastal ocean food web dynamics (Dunton *et al* 2012, McMeans *et al* 2013, Connelly *et al* 2015). Water yield (runoff) is a major control on DOC loaded into arctic rivers (Raymond *et al* 2007, Holmes *et al* 2012), and while the bulk of riverine DOC export occurs during the freshet, suprapermafrost groundwater flow can supply substantial quantities of DOC

to rivers and coastal waters during summer (Connolly *et al* 2020), when water and associated materials flow through seasonally thawed active layer soils. These direct subsurface flows help to support biological production during a time when riverine flow is relatively low.

Climate warming, permafrost thaw (Biskaborn *et al* 2019, Turetsky *et al* 2020), and hydrological cycle intensification (Rawlins *et al* 2010) are transforming Arctic environments, with changes in several linked processes likely to alter the terrestrial fluxes of DOC and other materials. Increasing river discharge (Arp *et al* 2020) should directly impact nutrient fluxes into Arctic coastal waters (Rood *et al* 2017). Indeed, recent studies have pointed to sustained long-term increases in DOC delivery to the Arctic Ocean and its marginal seas (McGuire *et al* 2010, Tank *et al* 2016). Observational studies in Siberia have shown a marked increase in the frequency of deep convective clouds capable of producing heavy summer rainfall (Chernokulsky *et al* 2011), and model studies suggest that convective precipitation may become more frequent in the future (Poujol *et al* 2020, 2021). In recent years, increasing warm season rainfall has caused an observed shift in the runoff regime of watersheds in northwest Alaska (Arp *et al* 2020). The increased magnitude and frequency of rainfall coupled with ongoing permafrost thaw has the potential to escalate the export of carbon from Arctic watersheds (Beel *et al* 2021).

In addition to the rainfall increases, other changes unfolding across northern Alaska and other parts of the Arctic have the potential to impact DOC exports to coastal zones. For example, studies have suggested that thawing permafrost is impacting the biogeochemistry and export characteristics of Arctic rivers (Striegl *et al* 2005, Frey *et al* 2007, Raymond *et al* 2007, Frey and McClelland 2009, Coch *et al* 2020). Permafrost, which is continuous across northwest Alaska, influences soil moisture by controlling vegetation and water drainage, especially in near-surface soils (Woo *et al* 2008, Walvoord *et al* 2012, Streletskiy *et al* 2017). Increased 'greening' of plant biomass has been reported in several recent observational studies using field data (Hill and Henry 2011, Elmendorf *et al* 2012) that have been corroborated by estimates of vegetation change obtained from satellite remote sensing (Bhatt *et al* 2010, Epstein *et al* 2012, Walker *et al* 2012) and numerical modeling (Epstein *et al* 2000, Euskirchen *et al* 2009). The satellite record indicates that greening has been prominent over the tundra of Alaska's North Slope (Jia *et al* 2003, Frost *et al* 2020). Yet, in the area near Utqiaġvik, there is evidence that some plant species have experienced an increase in biomass, while other species nearby showed decreased biomass from 1972 to 2008 (Goswami *et al* 2015), with the decreases potentially arising through landscape drying and/or biomass consumption by herbivores. A recent model study applied for Alaska's North Slope pointed to a significant increase in the proportion of subsurface runoff to total runoff for the region and for 24 of the 42 study basins, suggesting a physical connection between warming climate, permafrost degradation, and increasing subsurface flow to streams and rivers (Rawlins *et al* 2019). While numerous, it is not entirely clear how these change are impacting DOC exports. Moreover, the paucity of long-term measurements of DOC concentration in northern Alaska rivers hinders the quantification of fluvial DOC exports. In light of the data limitations, assessments that seek to characterize how the myriad changes unfolding across the region may be impacting freshwater and nutrient flows can benefit from the application of numerical models.

This study uses meteorological observations and a numerical model tailored to permafrost-dominated environments to investigate hydroclimatic trends and associated impacts to soil state conditions and, in turn, terrestrial freshwater and DOC exports to Elson Lagoon in northwest Alaska over the 40 year period 1981–2020. First, meteorological data are examined for the first and last five year intervals, followed by analysis of linear trends and significance over the full 40 year simulation period. Simulated soil temperature and moisture estimates are then explored to shed light on potential impacts of warming on production and export of DOC to the lagoon. Production and export of DOC from the contributing watershed, and directly along the lagoon's coastline, are then examined. Lastly, limitations of the model simulation and approaches are discussed. The overarching goal of this study is to provide a baseline of contemporary freshwater and DOC exports to Elson Lagoon against a backdrop of likely changes that have occurred over the past 40 years.

2. Methods

2.1. Model description, forcings, and parameterizations

This study focuses on terrestrial exports of freshwater and DOC to Elson Lagoon in northwest Alaska. The spatial domain encompasses the watershed that drains the small rivers and streams connecting to the lagoon. The 'Elson Watershed' is approximately 579 km^2 and is partitioned into 579 1×1 km grid cells (figure 1). A numerical model simulation was executed over the period 1981–2020 with the Permafrost Water Balance Model (v4) (figure S1 (available online at stacks.iop.org/ERL/16/105014/mmedia)). The transient 40-year simulation was preceded by a 50 year spinup on year 1980 to stabilize soil temperature, moisture, and soil DOC pools. Model parameterizations for soil texture, vegetation cover, and other static field are described in (Rawlins *et al* 2003, 2013). Vegetation across the watershed is exclusively tundra. While parameterizations for fields such as soil texture and vegetation cover are fundamental elements of land surface and hydrological

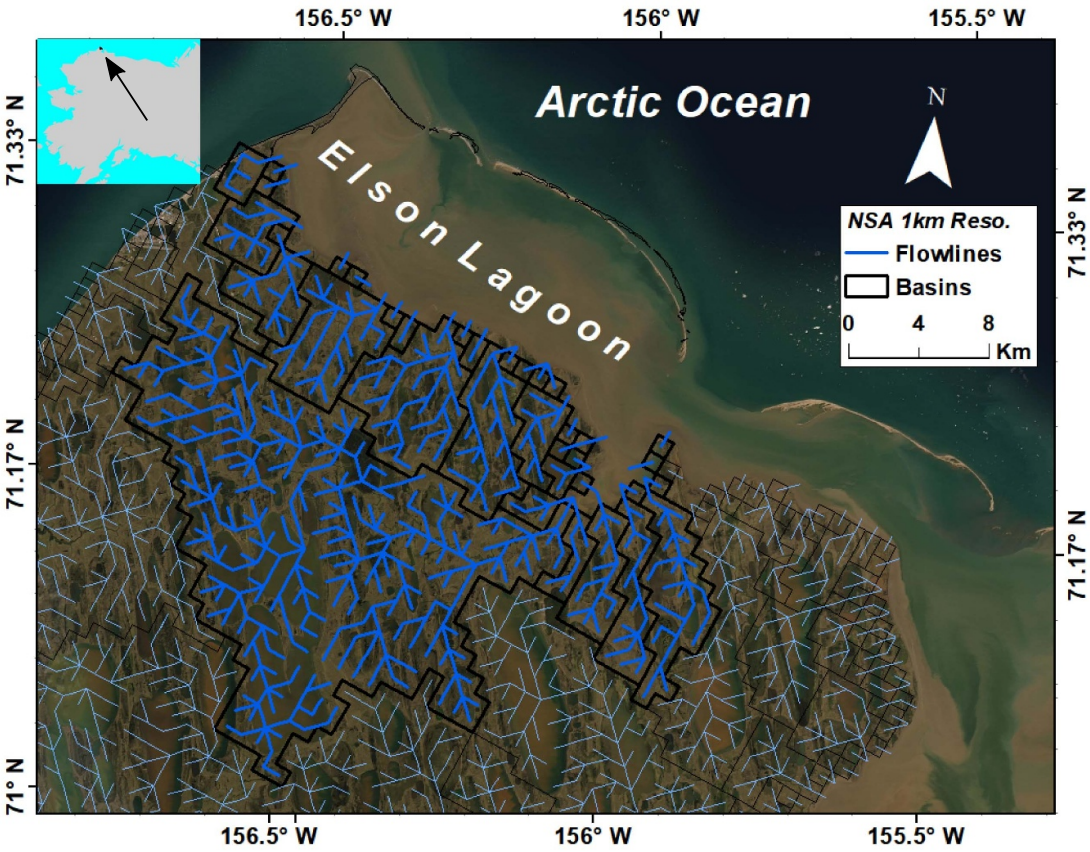

Figure 1. Map showing study focus area on the North Slope in northwest Alaska (NSA). Elson watershed indicated by darker blue flowlines (1 km resolution) connecting the drainage basin with Elson Lagoon. Simulated hydrology does not include processes involving or flow from the watershed's lakes and ponds.

model simulations, simulated runoff in Arctic regions is most sensitive to the time-varying meteorological forcings (Rawlins *et al* 2003). In the northern high latitudes a sparse station network often hinders confident assessment of the quality of gridded fields of near-surface (2 m) air temperature and precipitation necessary for model simulations across broad regions. This uncertainty is ameliorated in the present study through the use of meteorological observations at Utqiaġvik, Alaska, the most northerly first-order station (71.8189 °N, 156.8479 °W; 9.5 m ASL), in operation by the National Weather Service since 1901. Given the relatively flat terrain and small watershed size, daily 2 m air temperature, precipitation (available at http://climate.gi.alaska.edu/acis_data), and wind speed (available at https://mesonet.agron.iastate.edu) (table 1) were assigned to each of the watershed's grid cells.

The PWBM was recently updated to add process representations related to water loss from the surface and DOC production, decomposition, storage and loading to river networks (Rawlins *et al* 2021). Briefly, DOC production is influenced strongly by the amount of surface and soil organic matter and the dynamics of surface/soil temperature and moisture. A production rate coefficient (k_{prod}, table S1) is adjusted during calibration. The decomposition of DOC is assumed to result in losses to carbon dioxide and/or sorption to the mineral soil. As with production, a decomposition rate coefficient (k_{decomp}) is adjusted during calibration. Daily DOC production and loss to decomposition are used to update a soil DOC pool. Transfer of DOC from the surface or a soil layer to the stream and river network takes place whenever surface or subsurface runoff occurs:

$$DOC(t) = S_{DOC}(t)\, Q, \tag{1}$$

where $DOC(t)$ is mass loaded to a river network ($\mathrm{g\,C\,m^2\,day^{-1}}$), $S_{DOC}(t)$ is soilwater DOC storage ($\mathrm{g\,C\,m^{-3}}$), and Q is runoff ($\mathrm{m\,day^{-1}}$). Rawlins *et al* (2021) provide additional detail on the recent model updates.

Considerable uncertainty exists in the density of soil organic carbon in regional-scale simulations across Arctic environments. Given the relatively small extent of Elson Watershed, soil carbon density for each grid cell was assigned $50\,\mathrm{kg\,m^{-3}}$, which was the areally weighted mean amount calculated from soil cores collected along a transect within the watershed (Bockheim *et al* 1999), and is an approximate mid-point value between the 30 cm ($24\,\mathrm{kg\,m^{-3}}$) and 100 cm layer ($78\,\mathrm{kg\,m^{-3}}$) estimates for the area

Table 1. Primary data sets used in the model simulation.

Data set	Time period	Reference
Net primary productivity (NPP)[a]	1983–2005	Zhang *et al* (2009)
Surface meteorology[b]	1980–2020	DeGaetano *et al* (2015)
Surface water[c]	Average	Carroll *et al* (2016)

[a] Satellite-based efficiency model.
[b] Air temperature, precipitation, wind speed.
[c] 30 m data averaged to 1 km grids.

from the Northern Circumpolar Soil Carbon Database (Hugelius *et al* 2013).

The production, decomposition, and subsequent leaching of DOC into surface runoff is simulated in a similar manner to soil processes. In contrast to soil organic carbon, a surface carbon pool is parameterized as aboveground biomass from available data. This parameterization is important, as river sampling has consistently shown that DOC concentrations of North Slope and other arctic rivers peak during the spring freshet, when snowmelt-driven runoff leaches decaying tundra vegetation and organic-rich shallow soils above frozen ground, thereby mobilizing massive quantities of DOC that is shunted through fluvial networks (Spencer *et al* 2008, Holmes *et al* 2012, McClelland *et al* 2012). Aboveground carbon is parameterized here based on estimates of biomass from sites originally established near Utqiaġvik in 1972, and resampled in 1999, 2008 and 2012 (Lara *et al* 2012, Villarreal *et al* 2012). Biomass from the vegetation communities in these plots averages 49.9 $g\,C\,m^{-2}$ as reported by Goswami *et al* (2015). Parameterization of aboveground carbon storage is obtained by applying the rate increase derived from satellite-based estimates of net primary productivity (NPP) for the period 1985–2005 (available at http://files.ntsg.umt.edu/data/PA_Monthly_ET/) (table 1) (Zhang *et al* 2008) to the vegetation communities plots average set at its midpoint year 1992. Rawlins *et al* (2021) provide additional details of the model algorithms involving DOC production and leaching to streams and rivers.

The change analysis is focused on annual and seasonal riverine freshwater and DOC export totals. Recent evidence of hydrological cycle intensification and permafrost thaw across the region provide a basis for positing a null hypothesis of increasing freshwater and DOC flows to Elson Lagoon. Trend significance is assessed with the Mann–Kendall test (Mann 1945, Kendall 1955), with p-values below $p = 0.05$ considered to be statistically significant. Temporal autocorrelation for each time series examined was first assessed with the Durbin–Watson test (Durbin and Watson 1950), which involves the residuals from ordinary least squares regression:

$$D = \frac{\sum_{t=2}^{n}(e_t - e_{t-1})}{\sum_{t=1}^{n} e_t^2}, \quad (2)$$

where $e_t = y_t - \hat{y}_t$ are the residuals from the ordinary least squares fit of the y_t dependent variable, and $\hat{y}_t$ are the predicted values from the fitted linear regression model. The D test statistic values were compared with published tables of critical values to accept or reject the null hypothesis of no evidence of positive or negative autocorrelation at significance level $\alpha = 0.05$. None of the time series examined were found to exhibit positive serial autocorrelation, though the test was inconclusive for some variables. For surface and total DOC export, D values slightly above the critical value for negative autocorrelation imply a slight underestimation of the level of statistical significance. Given these results no transformations were performed on the variables examined.

2.2. Model validation

Measurements of river discharge from the small rivers and streams which drain to Elson Lagoon have only recently been made, and no long-term data for the area exist. In light of this shortcoming, the magnitude in simulated annual runoff is evaluated here against averages described in Arp *et al* (2020) for the Fish Creek Watershed, located approximately 200 km to the southeast. Simulated runoff averages of 91 (2001–2008), 129 (2009–2015), and 150 $mm\,yr^{-1}$ (2016–2019) compare favorably to the 90, 120, and 163 $mm\,yr^{-1}$ for Fish Creek, with percent differences of 1.1%, 7.5%, and 8%, respectively. This result suggests that the model simulation broadly captures the magnitude of freshwater export to Elson Lagoon. Similar model performance was demonstrated in a study of hydrological quantities estimated over the full North Slope drainage basin. For example, model simulated discharge for the Kuparuk River of 1.3 $km^3\,yr^{-1}$ (1981–2010) aligns with the observed annual total from USGS gauge data of 1.4 $km^3\,yr^{-1}$ (Rawlins *et al* 2019).

As with river discharge, there is a paucity of field observations of DOC concentration from streams and rivers that drain to the lagoon, particularly during the spring freshet, a shortcoming that hinders a robust validation of simulated DOC concentrations and associated DOC export. Here simulated DOC concentration for all rivers draining to the lagoon are compared to estimates for spring (May–June) and summer (July–September) that were derived from an empirical relationship between watershed slope and concentrations obtained from sampling of moderate and large Arctic rivers (Connolly *et al* 2018). The spring and summer periods were defined in Connolly *et al* (2018) to capture the spring (snowmelt-driven) freshet and subsequent summer low flows. Median simulated spring and summer DOC concentrations over years 2016–2020 of 24.3

and 8.2 mg C L^{-1}, respectively, are broadly consistent with the independent empirical averages of 18.0 and 13.2 mg C L^{-1} for the region. While the empirical estimates were obtained from a wide range of river measurements throughout the North Slope and other parts of Arctic, rivers across Northwest Alaska were relatively underrepresented in the construction of the empirical functions. Simulated concentrations of 5–10 mg C L^{-1} during late summer (late July to mid August) are also well within the range of 3–13 mg C L^{-1} obtained from sampling of small rivers near the lagoon at that time (Lougheed *et al* 2020).

End of season maximum active layer thickness (ALT) derived from simulated soil temperatures are congruent with data from the Circumpolar Active Layer Monitoring (CALM) program (available at https://www2.gwu.edu/calm/data/north.htm.) (Hinkel and Nelson 2003). Simulated ALT averaged across the watershed generally falls between the CALM observations for Barrow and Atkasuk (figure S2). For 2017 simulated ALT is in the upper half of the distribution of 30 m ALT from Remotely Sensed Active Layer Thickness (ReSALT) data (available at https://doi.org/10.3334/ORNLDAAC/1796) (Schaefer *et al* 2015). Each data series shows increasing ALT over time. Simulated ALTs are also consistent with the range reported in field studies (Nelson *et al* 1997, Hinkel *et al* 2001, Jafarov *et al* 2017).

3. Results and discussion

3.1. Climate trends

As with other parts of the Arctic, air temperatures in and around Utqiaġvik AK have warmed markedly over the past four decades. Since 1981 average temperatures have warmed significantly ($p < 0.01$) in all seasons (table 2, figure S3). Annual, winter, and spring average air temperatures have warmed at a rate of 1.1, 1.1, and 1.0 °C decade^{-1} ($p < 0.01$). Autumn has warmed by 2 °C decade^{-1}, nearly twice the rate of winter warming. The autumn temperature average is −3.5 °C over the most recent five year period 2016–2020. Given the long-term trend rate it is conceivable that a typical autumn will average above freezing by mid century. Summer also exhibits a significant positive trend, though considerably less (0.4 °C decade^{-1}) than the three other seasons.

Precipitation increases are noted in all seasons (table 2, figure S4), with the changes statistically significant for annual, winter, spring, and autumn totals. The trend in summer precipitation (5.1 mm decade^{-1}) falls just outside the level of statistical significance, though precipitation over the most recent 5 year period (2016–2020) is more than 50% greater than the first 5 years (1981–1985), consistent with other studies pointing to increasing rainfall rates across parts of the high northern latitudes and river discharge from watersheds approximately 200 km to the east of Elson Lagoon (Arp *et al* 2020). Precipitation over the latter period is nearly double the early average in winter, spring, and autumn, with percent changes of 103%, 85%, and 85% respectively. Annual total rainfall more than doubled between the first and last five years and increased significantly ($p < 0.001$) at a rate of 10.8 mm decade^{-1} over 1981–2020. Autumn shows the greatest rate of change for average air temperature (2.0 °C decade^{-1}). The rate increase in seasonal total precipitation is also highest in autumn (8.2 mm decade^{-1}). This accelerated change during autumn is an expected manifestation of the marked sea ice losses that have occurred in the nearby Beaufort and Chukchi Seas (Frey *et al* 2014, Steele *et al* 2015).

Table 2. Climate, hydrological, and DOC data for Elson Watershed. Averages are shown for first and last 5 year periods. Trend values are listed as per decade over the simulation period 1981–2020. Bold indicates trend significant at $p < 0.05$.

Variable	1981–1985	2016–2020	1981–2020
Air temperature (°C)			
Annual	−12.4	−7.8	**1.1**[a]
Winter	−24.2	−19.9	**1.1**[a]
Spring	−17.2	−12.3	**1.0**[a]
Summer	2.7	4.5	**0.4**[a]
Autumn	−11.0	−3.5	**2.0**[a]
Precipitation (mm)			
Annual	115	200	**23.1**[b]
Winter	13.1	28.5	**4.2**[b]
Spring	15.8	29.2	**5.3**[b]
Summer	55.0	83.9	5.1[b]
Autumn	31.7	58.7	**8.2**[b]
Annual rainfall (mm)	48	102	**10.8**[b]
Runoff (mm)			
Total	79.9	138.5	**17.7**[b]
Surface	47.4	76.3	**11.7**[b]
Subsurface	32.5	62.3	**6.0**[b]
DOC production (g C m^{-2})			
Surface	1.23	2.48	**0.33**[c]
Subsurface	1.27	1.99	**0.17**[c]
DOC export (Mg C)			
Total	794	1270	**123**[d]
Surface	513	866	**97**[d]
Subsurface	281	406	**26**[d]
Coastal freshwater export (m^3)			
Subsurface, August–October	6.4×10^5	1.7×10^6	**2.2×10^5**[e]
Coastal DOC flux (kg C)			
Subsurface, August–October	6180	13 030	**1335**[f]

[a] °C decade^{-1}.
[b] mm decade^{-1}.
[c] g C m^{-2} decade^{-1}.
[d] Mg C decade^{-1}.
[e] m^3 decade^{-1}.
[f] kg C decade^{-1}.

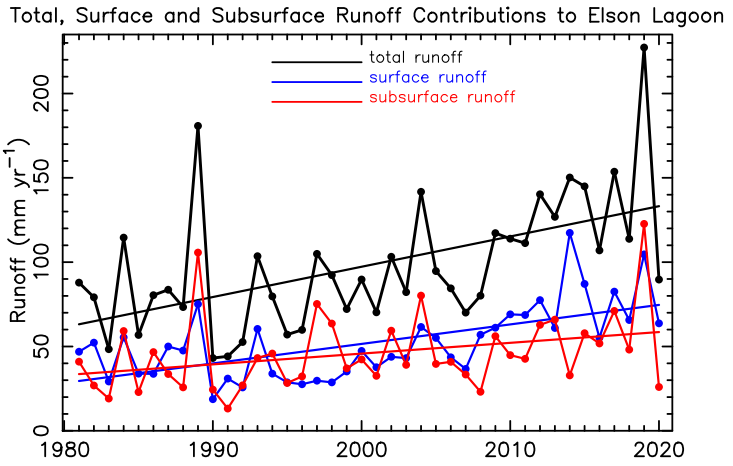

Figure 2. Surface, subsurface, and total runoff contributions (mm yr^{-1}) to Elson Lagoon over the 40 year simulation period 1981–2020. Linear least squares trends shown.

3.2. Runoff and freshwater export trends

Over the simulation period 1981–2020, increases in surface and subsurface runoff across the contributing watershed are evident (figure 2). The increases in runoff—17.7, 11.7, and 6.0 mm decade^{-1} for total, surface, and subsurface runoff, respectively (table 2)—and associated freshwater export to Elson Lagoon are consistent with recent increases in discharge from rivers in the Fish Creek Watershed (Arp *et al* 2020). In particular, the excessive amount of subsurface runoff in 2019 (126 mm) aligns with the highest runoff reported for Fish Creek Watershed's rivers over the 2001–2019 period examined in that study. These trends point to hydrologic cycle intensification manifesting in increased freshwater export to Elson Lagoon and nearby parts of Northwest Alaska.

3.3. Soil temperature and moisture

Organic carbon stored in tundra regions is highly vulnerable to decomposition through warming-induced thaw of permafrost (Xue *et al* 2016, Feng *et al* 2020). Organic carbon in the active layer is also vulnerable to increased decomposition rates under warmer conditions. Soil temperatures near Elson Lagoon have warmed markedly over recent decades. For example, for a representative grid in the watershed, soil temperature at 13 cm depth between DOY 170 and 240 averaged 0 °C in 1983 and 4 °C in 2019 (figure 3). Soil temperature at 23 cm remained near 0 °C during summer in 1983, a result of the 'zero curtain', the effect of latent heat maintaining temperatures near 0 °C over extended periods. In 2019 soil temperature at 23 cm averaged 3 °C, with thaw at the end of summer reaching close to 50 cm. Assuming that the active layer extends to the depth at which soil temperature equals 0 °C, maximum ALT, as an average of all of the watershed's grids, averaged 28.5 cm over the simulation's first five years (1981–1985) and 45.8 cm over the last five years (2016–2020) (figure S2). The trend over the full 40 year period is statistically significant ($p < 0.001$) for all grids, averaging 4.0 cm decade^{-1} (s.d. 0.51 decade^{-1}). Soil moisture in the thawed active layer reflects the influence of climate warming. For example, in the years 1981–1983, nearly saturated soil is present through the profile during the first few weeks after thaw and in the lower half of the profile in late summer (figure 4(a)). The active layer extends to a depth of 20 cm in 1981 and 1982, and only 10 cm in 1983. The simulation shows a much deeper depth of thaw in 2017–2019 (figure 4(b)). In the latter period thaw extends to roughly 40, 30, and 50 cm in 2017, 2018, and 2019 respectively. Soil water content increases from the surface downward, consistent with field measurements that captured water pooling above the permafrost (Hinzman and Kane 1991). This gradient expressed in the model simulation is expected, and noted in the earlier period as well, though not as pronounced given the shallower depth of thaw. Surface warming along with drainage into a deeper profile contribute to enhanced drying of near surface soils near the end of summer in more recent years. Warmer soils and a larger volume of thawed material manifest in a trend to greater production of DOC in the subsurface flow (figure 5(a)).

3.4. DOC production and export

The production of DOC in soils varies with SOC content, and is sensitive to soil temperature and moisture. Simulated production is low in winter when soils are cold and there is little or no liquid water present (figure S5(a)). During the warm season production varies by a factor of five, and is highest when the temperature of a model soil layer approaches 15 °C, and it is nearly water saturated, averaging approximately 10 mg C day^{-1} during these conditions. The simulation demonstrates how the magnitude of DOC leachate that contributes to stream loadings is lowest when the soil water DOC pool is at the low end of its range, and when the concentration of the leachate is low (figure S5(b)). Conversely, leachate magnitudes

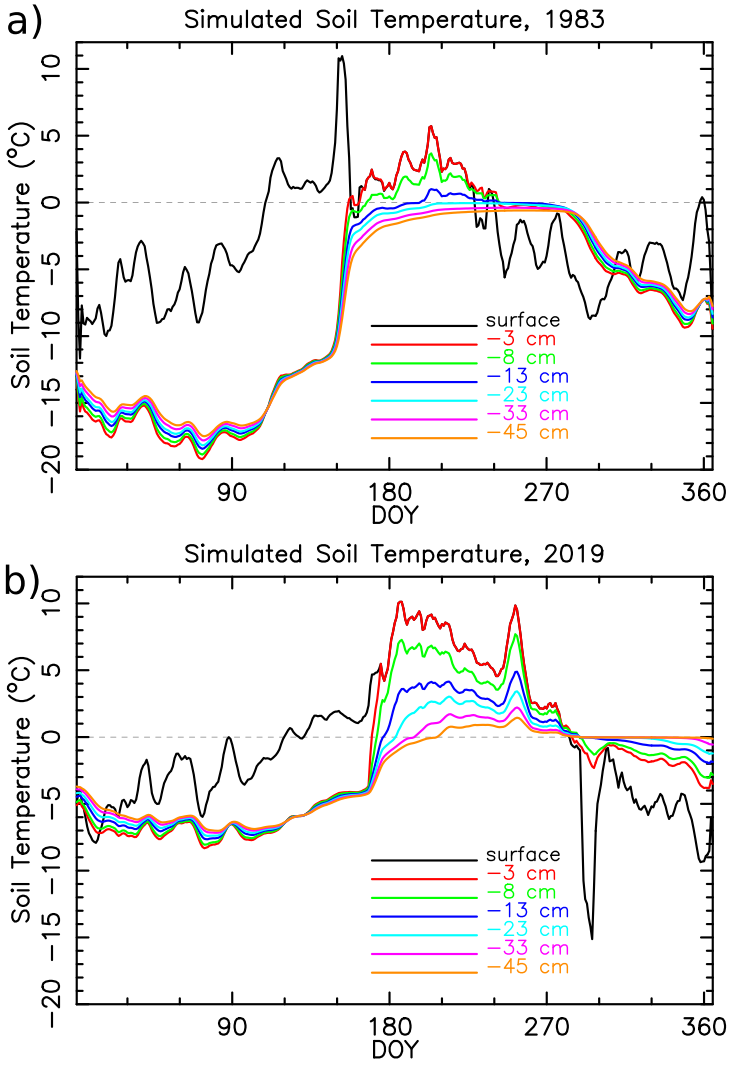

Figure 3. Daily soil temperatures (°C) for single grid cell in the center of Elson basin for years: (a) 1983 and (b) 2019. Soil temperatures shown for seven of the 23 model layers, with the center of the layers at the surface and depths −3, −8, −13, −23, −33, −45 cm.

are highest when soil water DOC storage and leachate concentrations are high, exceeding at times the daily production rate, particularly when soils are nearly saturated during runoff events, for example, during or following heavy rains in the warmth of late summer (figure S6). Soil water DOC storage decreases sharply in late spring during flushing events to roughly half its magnitude prior to the freshet. Production of DOC in summer increases the storage pool, with the change in magnitude reflecting both production and decomposition. The storage pool also increases during winter, though influenced then by much lower rates of production and decomposition, relative to summer.

Over the past 40 years, DOC production at the surface and in soils increased ($p < 0.01$), with subsurface production exhibiting a slightly higher level of significance given lower interannual variability relative to the surface (figure 5). Simulated total DOC export to the lagoon likewise increased ($p < 0.01$), driven by increases from loading in surface ($p < 0.01$) and suprapermafrost flow ($p = 0.01$). The rate of change is slightly greater for surface export (table 2), owing to the influences of warming (figure S3(c)) and increasing biomass and surface runoff (figure 2). Significantly higher amounts of DOC flux in the suprapermafrost subsurface flow are noted in the more recent five year period relative to the past (figure 6). The change is greatest in late summer-fall. DOC export from suprapermafrost flow has increased in all months, except for June. Some 119.5 and 536.7 Mg DOC was exported in September and October during 1981–1985 and 2016–2020, respectively, an increase of 450%. Daily mean export from suprapermafrost flow is now higher from June through September. Percent differences between the two periods range from 7.5% for July to 49.5% in September. There are now more days in May with DOC export from suprapermafrost flow (two in 1981–1985 vs. ten in 2016–2020), and many more days in October (three vs. ninety-eight). Suprapermafrost flow is now emerging in November. The changes in subsurface processes

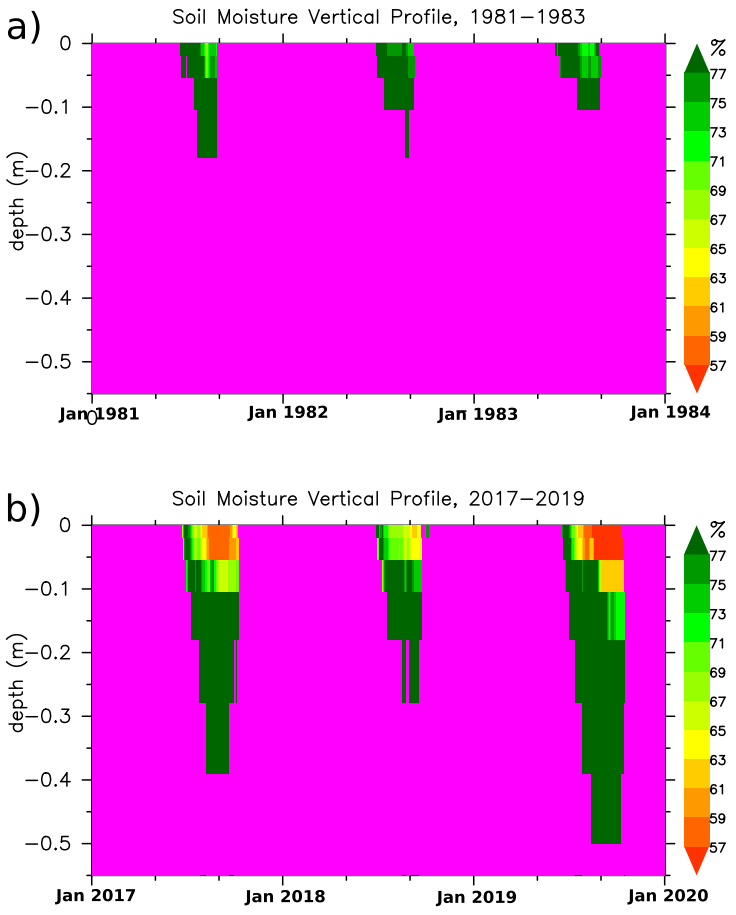

Figure 4. Daily soil moisture volumetric water content (%) through a vertical profile for grid cell shown in figure 4 for years: (a) 1981–1983 and (b) 2017–2019. Magenta shading indicates soil temperatures at or below 0 °C.

arise as a result of warmer soils, a greater volume of thawed soils, and increasing subsurface runoff.

Approximately 34 km of coastline border Elson Lagoon. Subsurface flow along the coastal zone during summer provides a direct transfer of freshwater and DOC to the lagoon through the thawed active layer. The simulation indicates that late summer (August–October) suprapermafrost coastline freshwater export directly to the lagoon averages 6.4×10^5 m^3 during 1981–1985 and 1.7×10^6 m^3 during 2016–2020 (table 2), an increase of ∼165%. A massive flux anomaly of 3.3×10^6 m^3 in 2019 is a factor of four greater than the early 1980s average. Suprapermafrost coastal DOC export directly to the lagoon during late summer 1981–1985 varied from 3950–10 040 kg DOC, averaging 6180 kg C. In 2016–2020 this increased to 8280–23 840 kg C, with the highest amount exported in 2019. The 5 year average is 13 030 kg C, more than double (111%) the late summer export amount during the early period. The late summer total in 2019 represents an increase of 285% from 1981 to 1985 period average. September experienced the largest increases, with coastal suprapermafrost DOC export in 2019 (8906 kg C) a more than fourfold increase (459%) over the average during 1981–1985.

4. Study limitations

This study illustrates how climate warming, thawing permafrost, and higher precipitation rates have increased DOC export to Elson Lagoon. While the model employed here is well suited for analysis of temporal changes in surface and subsurface hydrology and carbon leaching from surface and subsurface carbon pools, there are aspects of the model simulation to bear in mind. For example, while studies from field and remote sensing data and models have pointed to greening of tundra vegetation (Zhang *et al* 2008, Bhatt *et al* 2010, Hill and Henry 2011, Elmendorf *et al* 2012), observations of biomass in plots near the lagoon show increases for some plant species and decreases for others (Goswami *et al* 2015). The positive trend in simulated surface DOC production and subsequent export reflects a multi-decadal increase in tundra biomass that is impossible to verify with a high degree of certainty. While a longer growing season and increases in nutrients released from thawing permafrost (Lougheed *et al* 2015) are know to influence enhanced vegetation productivity across northern Alaska, a high degree of uncertainty surrounds the changes in simulated surface DOC production,

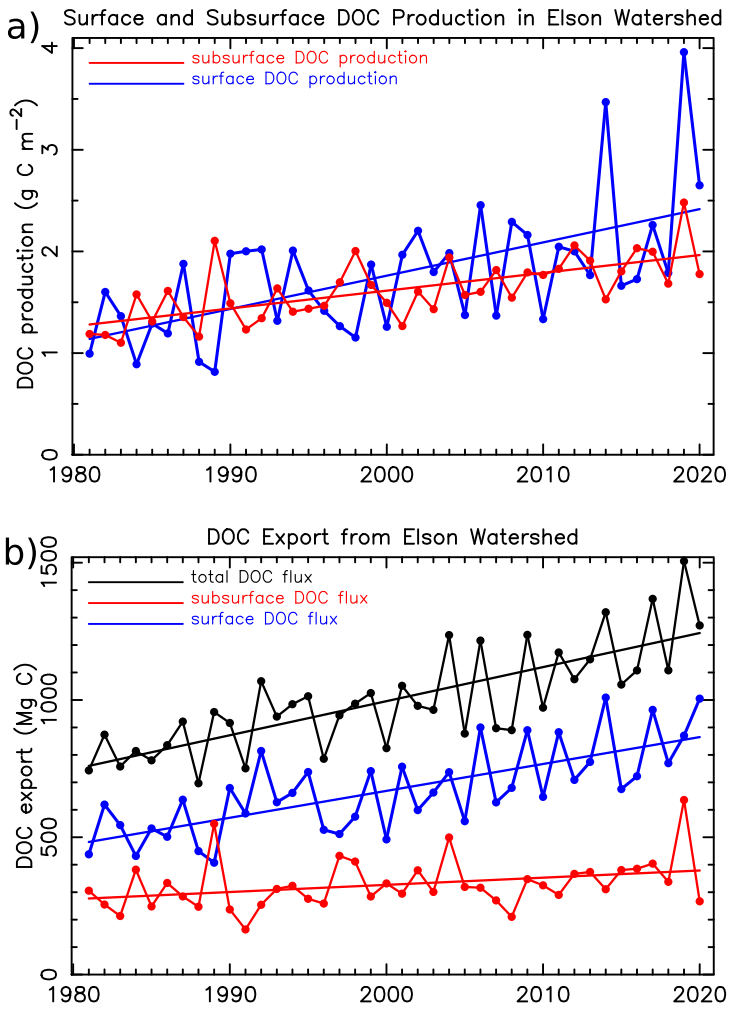

Figure 5. (a) Annual total DOC production at the surface (blue) and within the soil profile (subsurface, red) as an average across the Elson watershed. (b) Total DOC export to Elson Lagoon (black), the sum of DOC loaded from the surface (blue) and subsurface (red).

leaching, and export reported here. These uncertainties highlight the need for studies that evaluate interactions and responses of tundra vegetation to ongoing environmental changes in this region.

Numerous ponds and small lakes are present in Elson Watershed. While the model includes a lake module that accounts for precipitation inputs, evaporative losses, and associated changes in storage, it does not simulate the influence of any hydrologically-connected waterbodies on the simulated DOC totals in this study. Incorporating DOC export from ponds to streams is a particular challenge in this region, as many of the surface water bodies have no discernible connection to a nearby stream. This uncertainty in model parameterization supports the need for studies that characterize the transfer of DOC from surface water bodies to stream and river networks and the parallel development of models that quantify the production and in-situ processing of DOC in these surface features. The role of surface waters in riverine DOC export is important to consider, at least for large lakes, as there is emerging evidence that increasing DOC exports from the Mackenzie River may be resulting from processes within Great Bear Lake (Tank *et al* 2016). Development and implementation of models that characterize the influences of lakes in riverine DOC exports in northwest Alaska will require new information on connections between surface water bodies and stream networks, along with a better understanding of key processes controlling in-situ carbon production and decomposition. The DOC exports estimated here do not account for in-stream processing (Cory *et al* 2014), though such losses from photo- and microbial degradation in the water column may be limited given the short travel times in this small watershed. Future field studies of water temperature, oxygen saturation, DOC concentration, and other relevant quantities will aid in the development, testing, and implementation of models which quantify rates of in-stream processing. Studies of DOC processing for the Kuparuk River (Holmes *et al* 2008, Rocher-Ros *et al* 2021) and regional-scale estimates of carbon fluxes for inland aquatic ecosystems in Alaska (Stackpoole *et al* 2017) suggest that lateral exports are less than the leachate loadings to rivers.

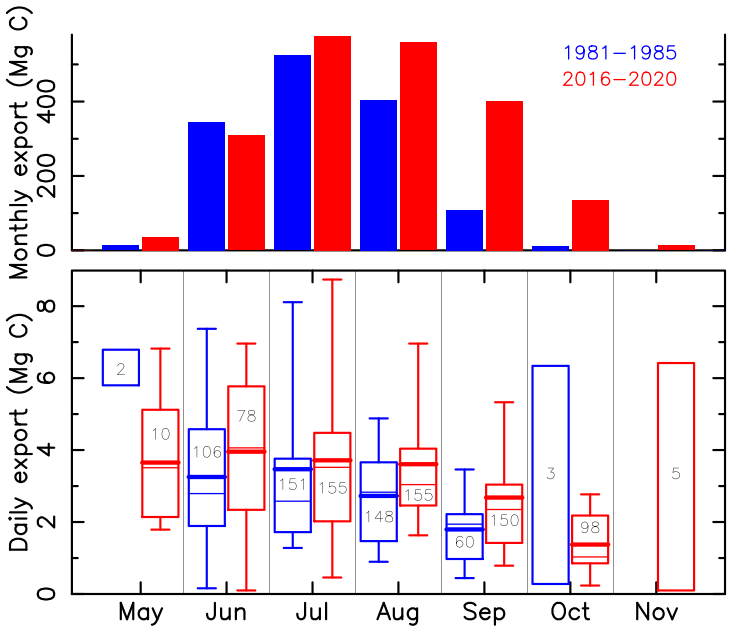

Figure 6. Barchart showing simulated DOC export via suprapermafrost flow as a total (Mg (C) for months May to November for periods 1981–1985 and 2016–2020. Box plots shows the distribution of average daily DOC export to Elson Lagoon via suprapermafrost flow during the periods. Boxplot rectangles bracket the 25th and 75th percentiles. Whiskers extend to the 5th and 95th percentiles. Thick and thin horizontal lines mark the distribution mean and median respectively. Rectangles without whiskers span the range of the maximum and minimum daily mean export values. The number in each box is the total number of days with suprapermafrost flow each month over the respective period.

The estimates described here do not account for direct fluxes of soil organic matter to the lagoon from coastal erosion. Historic rates of erosion near Elson Lagoon are ∼1–2 m per year, considerably lower than other areas of the Beaufort Sea coast that lack protection from barrier islands (Gibbs and Richmond 2017, Jones *et al* 2018). Nonetheless, erosion is an important component of organic carbon mass exports, particularly on decadal timescales. The simulation also does not capture localized effects on carbon mobilization and transport, such as thermokarst lake drainage (Jones and Arp 2015), land subsidence (Streletskiy *et al* 2017, Coch *et al* 2020), rapid surface-subsurface exchanges (Neilson *et al* 2018), and hillslope water tracks (Rushlow and Godsey 2017, Walvoord *et al* 2019, Evans *et al* 2020), though the latter process is unlikely to play a significant role given the watershed's relatively flat terrain. Frequent sampling of the region's small streams is critical to more rigorous calibration and validation of numerical models.

5. Conclusions

This study describes a decades long trend in freshwater and DOC export to Elson Lagoon, quantified by a model simulation, that supports the hypothesis of increasing fluxes, and adds to a growing body of evidence that hydrologic cycle intensification and permafrost thaw are impacting coastal ecosystems in northern Alaska. Results suggest that increasing rates of DOC production and export in subsurface suprapermafrost flows are being driven by warming and associated increases in the volume of thawed permafrost soils. The greatest monthly change between the first and last five years of the simulation in DOC export attributed to suprapermafrost flows is noted in September, which has experienced an increase of nearly 50%. Suprapermafrost flows of DOC now occurs more frequently in October, and takes place in November, which had no subsurface runoff during the early 1980s. The simulation also suggests that, along the coastal zone bordering the lagoon, suprapermafrost freshwater flow in late summer has increased. An extraordinarily large anomaly in September 2019 represents a more than fourfold departure from the September average in 1981–1985. High rates of change in surface climate during autumn highlight the need for dedicated efforts to gather observations connected to processes controlling DOC production, leaching, and subsequent export well after field season typically concludes.

Data availability statement

The data that support the findings of this study are openly available at the following URL/DOI: Long Term Ecological Research (LTER) Network Data Portal at https://doi.org/10.6073/pasta/a49b3da18b4c83d6ff69d9d878bb7dc3. Model available at https://blogs.umass.edu/csrc/pwbm/.

Acknowledgments

Raymond Bradley and James McClelland are thanked for comments on an earlier version of the manuscript. Shahab Afshari and Timothy Whiteaker are thanked for providing technical assistance. This work was supported by funding from the U.S. Department of Energy, Office of Biological and Environmental Research (Grant No. DE-SC0019462), the National Aeronautics and Space Administration (Grant No. 80NSSC19K0649), and the National Science Foundation, Division of Polar Programs (Grant No. NSF-OPP-1656026).

ORCID iD

Michael A Rawlins https://orcid.org/0000-0002-3323-8256

References

Arp C, Whitman M, Kemnitz R and Stuefer S 2020 Evidence of hydrological intensification and regime change from northern Alaskan watershed runoff *Geophys. Res. Lett.* **47** e2020GL089186

Beel C, Heslop J, Orwin J, Pope M, Schevers A, Hung J, Lafrenière M and Lamoureux S 2021 Emerging dominance of summer rainfall driving High Arctic terrestrial-aquatic connectivity *Nat. Commun.* **12** 1–9

Bhatt U S *et al* 2010 Circumpolar Arctic tundra vegetation change is linked to sea ice decline *Earth Interact.* **14** 1–20

Biskaborn B K *et al* 2019 Permafrost is warming at a global scale *Nat. Commun.* **10** 1–11

Bockheim J, Everett L, Hinkel K, Nelson F and Brown J 1999 Soil organic carbon storage and distribution in arctic tundra, Barrow, Alaska *Soil Sci. Soc. Am. J.* **63** 934–40

Box J E *et al* 2019 Key indicators of Arctic climate change: 1971–2017 *Environ. Res. Lett.* **14** 045010

Carroll M, Wooten M, DiMiceli C, Sohlberg R and Kelly M 2016 Quantifying surface water dynamics at 30 meter spatial resolution in the North American high northern latitudes 1991–2011 *Remote Sens.* **8** 622

Chernokulsky A, Bulygina O and Mokhov I 2011 Recent variations of cloudiness over Russia from surface daytime observations *Environ. Res. Lett.* **6** 035202

Coch C, Ramage J L, Lamoureux S F, Meyer H, Knoblauch C and Lantuit H 2020 Spatial variability of dissolved organic carbon, solutes and suspended sediment in disturbed low Arctic coastal watersheds *J. Geophys. Res.: Biogeosci.* **125** e2019JG005505

Connelly T L, McClelland J W, Crump B C, Kellogg C T and Dunton K H 2015 Seasonal changes in quantity and composition of suspended particulate organic matter in lagoons of the Alaskan Beaufort Sea *Mar. Ecol. Prog. Ser.* **527** 31–45

Connolly C T, Cardenas M B, Burkart G A, Spencer R G and McClelland J W 2020 Groundwater as a major source of dissolved organic matter to Arctic coastal waters *Nat. Commun.* **11** 1–8

Connolly C T, Khosh M S, Burkart G A, Douglas T A, Holmes R M, Jacobson A D, Tank S E and McClelland J W 2018 Watershed slope as a predictor of fluvial dissolved organic matter and nitrate concentrations across geographical space and catchment size in the Arctic *Environ. Res. Lett.* **13** 104015

Cory R M, Ward C P, Crump B C and Kling G W 2014 Sunlight controls water column processing of carbon in arctic fresh waters *Science* **345** 925–8

DeGaetano A T, Noon W and Eggleston K L 2015 Efficient access to climate products using ACIS web services *Bull. Am. Meteorol. Soc.* **96** 173–80

Dunton K H, Schonberg S V and Cooper L W 2012 Food web structure of the Alaskan nearshore shelf and estuarine lagoons of the Beaufort Sea *Estuaries Coasts* **35** 416–35

Durbin J and Watson G S 1950 Testing for serial correlation in least squares regression I *Biometrika* **37** 409–28

Elmendorf S C *et al* 2012 Plot-scale evidence of tundra vegetation change and links to recent summer warming *Nat. Clim. Change* **2** 453–7

Epstein H E, Raynolds M K, Walker D A, Bhatt U S, Tucker C J and Pinzon J E 2012 Dynamics of aboveground phytomass of the circumpolar Arctic tundra during the past three decades *Environ. Res. Lett.* **7** 015506

Epstein H E, Walker M D, Chapin III F S and Starfield A M 2000 A transient, nutrient-based model of arctic plant community response to climatic warming *Ecol. Appl.* **10** 824–41

Euskirchen E S, McGuire A D, Chapin III F S Y S and Thompson C C 2009 Changes in vegetation in northern Alaska under scenarios of climate change, 2003–2100: implications for climate feedbacks *Ecol. Appl.* **19** 1022–43

Evans S G, Godsey S E, Rushlow C R and Voss C 2020 Water tracks enhance water flow above permafrost in upland Arctic Alaska hillslopes *J. Geophys. Res.: Earth Surface* **125** e2019JF005256

Feng J *et al* 2020 Warming-induced permafrost thaw exacerbates tundra soil carbon decomposition mediated by microbial community *Microbiome* **8** 1–12

Frey K E, Maslanik J A, Kinney J C and Maslowski W 2014 Recent variability in sea ice cover, age and thickness in the Pacific Arctic region *The Pacific Arctic Region: Ecosystem Status and Trends in a Rapidly Changing Environment* ed J M Grebmeier and W Maslowski (Dordrecht: Springer) pp 31–63

Frey K E and McClelland J W 2009 Impacts of permafrost degradation on arctic river biogeochemistry *Hydrol. Process.* **23** 169–82

Frey K E, McClelland J W, Holmes R M and Smith L C 2007 Impacts of climate warming and permafrost thaw on the riverine transport of nitrogen and phosphorus to the Kara Sea *J. Geophys. Res.: Biogeosci.* **112** G04S58

Frost G V *et al* 2020 Tundra greenness *Arctic Report Card 2020* ed R L Thoman, J Richter-Menge and M L Druckenmiller (DIANE Publishing) (https://doi.org/10.25923/46rm-0w23)

Gibbs A E and Richmond B M 2017 National assessment of shoreline change—Summary statistics for updated vector shorelines and associated shoreline change data for the north coast of Alaska, U.S.–Canadian border to Icy Cape: U.S. Geological Survey Open-File Report 2017–1107 *Tech. Rep.* (U.S. Geological Survey)

Goswami S, Gamon J, Vargas S and Tweedie C 2015 Relationships of NDVI, Biomass, and Leaf Area Index (LAI) for six key plant species in Barrow, Alaska *Technical Report* PeerJ PrePrints

Hill G B and Henry G H 2011 Responses of High Arctic wet sedge tundra to climate warming since 1980 *Glob. Change Biol.* **17** 276–87

Hinkel K and Nelson F 2003 Spatial and temporal patterns of active layer thickness at Circumpolar Active Layer Monitoring (CALM) sites in northern Alaska, 1995–2000 *J. Geophys. Res.: Atmos.* **108** 8168

Hinkel K, Paetzold F, Nelson F and Bockheim J 2001 Patterns of soil temperature and moisture in the active layer and upper permafrost at Barrow, Alaska: 1993–1999 *Glob. Planet. Change* **29** 293–309

Hinzman L D and Kane D L 1991 Snow hydrology of a headwater Arctic Basin 2. Conceptual analysis and computer modeling *Water Resour. Res.* **27** 1111–21

Holland M M and Bitz C M 2003 Polar amplification of climate change in coupled models *Clim. Dyn.* **21** 221–32
Holmes R M *et al* 2012 Seasonal and annual fluxes of nutrients and organic matter from large rivers to the Arctic Ocean and surrounding seas *Estuaries Coasts* **35** 369–82
Holmes R M, McClelland J W, Raymond P A, Frazer B B, Peterson B J and Stieglitz M 2008 Lability of DOC transported by Alaskan rivers to the Arctic Ocean *Geophys. Res. Lett.* **35** L03402
Hugelius G, Tarnocai C, Broll G, Canadell J, Kuhry P and Swanson D 2013 The Northern Circumpolar Soil Carbon Database: spatially distributed datasets of soil coverage and soil carbon storage in the northern permafrost regions *Earth Syst. Sci. Data* **5** 3–13
Jafarov E, Parsekian A, Schaefer K, Liu L, Chen A, Panda S and Zhang T 2017 Estimating active layer thickness and volumetric water content from ground penetrating radar measurements in Barrow, Alaska *Geosci. Data J.* **4** 72–9
Jia G J, Epstein H E and Walker D A 2003 Greening of arctic Alaska, 1981–2001 *Geophys. Res. Lett.* **30** 2067
Jones B M *et al* 2018 A decade of remotely sensed observations highlight complex processes linked to coastal permafrost bluff erosion in the Arctic *Environ. Res. Lett.* **13** 115001
Jones B M and Arp C D 2015 Observing a catastrophic thermokarst lake drainage in northern Alaska *Permafr. Periglac. Process.* **26** 119–28
Kendall M G 1955 *Rank Correlation Methods 1955* (London: Charles Griffin & Co. Ltd)
Lara M, Villarreal S, Johnson D, Hollister R, Webber P and Tweedie C 2012 Estimated change in tundra ecosystem function near Barrow, Alaska between 1972 and 2010 *Environ. Res. Lett.* **7** 015507
Lougheed V L, Hernandez C, andresen C G, Miller N A, Alexander V and Prentki R 2015 Contrasting responses of phytoplankton and benthic algae to recent nutrient enrichment in Arctic tundra ponds *Freshw. Biol.* **60** 2169–86
Lougheed V L, Tweedie C E, andresen C G, Armendariz A M, Escarzaga S M and Tarin G 2020 Patterns and drivers of carbon dioxide concentrations in aquatic ecosystems of the Arctic coastal tundra *Glob. Biogeochem. Cycles* **34** e2020GB006552
Mann H B 1945 Nonparametric tests against trend *Econometrica* **13** 245–59
McClelland J W, Holmes R M, Dunton K H and Macdonald R W 2012 The Arctic Ocean Estuary *Estuaries Coasts* **35** 353–68
McClelland J W, Townsend-Small A, Holmes R M, Pan F, Stieglitz M, Khosh M and Peterson B J 2014 River export of nutrients and organic matter from the North Slope of Alaska to the Beaufort Sea *Water Resour. Res.* **50** 1823–39
McGuire A D *et al* 2010 An analysis of the carbon balance of the Arctic Basin from 1997 to 2006 *Tellus* B **62** 455–74
McMeans B C, Rooney N, Arts M T and Fisk A T 2013 Food web structure of a coastal Arctic marine ecosystem and implications for stability *Mar. Ecol. Prog. Ser.* **482** 17–28
Neilson B T, Cardenas M B, O'Connor M T, Rasmussen M T, King T V and Kling G W 2018 Groundwater flow and exchange across the land surface explain carbon export patterns in continuous permafrost watersheds *Geophys. Res. Lett.* **45** 7596–605
Nelson F E, Shiklomanov N I, Mueller G R, Hinkel K M, Walker D A and Bockheim J G 1997 Estimating active-layer thickness over a large region: Kuparuk River Basin, Alaska, U.S.A. *Arct. Alp. Res.* **29** 367–78
Poujol B, Prein A F, Molina M J and Muller C 2021 Dynamic and thermodynamic impacts of climate change on organized convection in Alaska. *Climate Dynamics* 56 2569–93
Poujol B, Prein A F and Newman A J 2020 Kilometer-scale modeling projects a tripling of Alaskan convective storms in future climate *Clim. Dyn.* **55** 3543–64
Rawlins M A *et al* 2010 Analysis of the Arctic system for freshwater cycle intensification: observations and expectations *J. Clim.* **23** 5715–37
Rawlins M A 2021 Model estimates of hydrological, dissolved organic carbon, soil temperature and moisture for Elson Lagoon watershed, Alaska, 1981-2020 (available at: https://doi.org/10.6073/pasta/a49b3da18b4c83d6ff69d9d878bb7dc3)
Rawlins M A, Cai L, Stuefer S L and Nicolsky D J 2019 Changing characteristics of runoff and freshwater export from watersheds draining northern Alaska *Cryosphere* **13** 3337–52
Rawlins M A, Connolly C T and McClelland J W 2021 Modeling terrestrial dissolved organic carbon loading to western Arctic rivers *J. Geophys. Res. Biogeo.* **126** e2021JG006420
Rawlins M A, Lammers R B, Frolking S, Fekete B M and Vörösmarty C J 2003 Simulating Pan-Arctic runoff with a macro-scale terrestrial water balance model *Hydrol. Process.* **17** 2521–39
Rawlins M A, Nicolsky D J, McDonald K C and Romanovsky V E 2013 Simulating soil freeze/thaw dynamics with an improved pan-Arctic water balance model *J. Adv. Model. Earth Sys.* **5** 659–75
Raymond P A, McClelland J W, Holmes R M, Zhulidov A V, Mull K, Peterson B J, Striegl R G, Aiken G R and Gurtovaya T Y 2007 Flux and age of dissolved organic carbon exported to the Arctic Ocean: a carbon isotopic study of the five largest arctic rivers *Glob. Biogeochem. Cycles* **21** GB4011
Rocher-Ros G, Harms T K, Sponseller R A, Väisänen M, Mörth C-M and Giesler R 2021 Metabolism overrides photo-oxidation in CO_2 dynamics of Arctic permafrost streams *Limnol. Oceanogr.* **66** S169–81
Rood S B, Kaluthota S, Philipsen L J, Rood N J and Zanewich K P 2017 Increasing discharge from the Mackenzie River system to the Arctic Ocean *Hydrol. Process.* **31** 150–60
Rushlow C R and Godsey S E 2017 Rainfall–runoff responses on Arctic hillslopes underlain by continuous permafrost, North Slope, Alaska, USA *Hydrol. Process.* **31** 4092–106
Schaefer K *et al* 2015 Remotely sensed active layer thickness (ReSALT) at Barrow, Alaska using interferometric synthetic aperture radar *Remote Sens.* **7** 3735–59
Serreze M C, Barrett A P, Stroeve J C, Kindig D N and Holland M M 2009 The emergence of surface-based Arctic amplification *Cryosphere* **3** 1–19
Spencer R G, Aiken G R, Wickland K P, Striegl R G and Hernes P J 2008 Seasonal and spatial variability in dissolved organic matter quantity and composition from the Yukon River basin, Alaska *Glob. Biogeochem. Cycles* **22** GB4002
Stackpoole S M, Butman D E, Clow D W, Verdin K L, Gaglioti B V, Genet H and Striegl R G 2017 Inland waters and their role in the carbon cycle of Alaska *Ecol. Appl.* **27** 1403–20
Steele M, Dickinson S, Zhang J and Lindsay W R 2015 Seasonal ice loss in the Beaufort Sea: toward synchrony and prediction *J. Geophys. Res.: Oceans* **120** 1118–32
Streletskiy D A, Shiklomanov N I, Little J D, Nelson F E, Brown J, Nyland K E and Klene A E 2017 Thaw subsidence in undisturbed tundra landscapes, Barrow, Alaska, 1962–2015 *Permafr. Periglac. Process.* **28** 566–72
Striegl R G, Aiken G R, Dornblaser M M, Raymond P A and Wickland K P 2005 A decrease in discharge-normalized DOC export by the Yukon River during summer through autumn *Geophys. Res. Lett.* **32** L21413
Tank S E, Striegl R G, McClelland J W and Kokelj S V 2016 Multi-decadal increases in dissolved organic carbon and alkalinity flux from the Mackenzie drainage basin to the Arctic Ocean *Environ. Res. Lett.* **11** 054015
Turetsky M R *et al* 2020 Carbon release through abrupt permafrost thaw *Nat. Geosci.* **13** 138–43
Villarreal S, Hollister R, Johnson D, Lara M, Webber P and Tweedie C 2012 Tundra vegetation change near Barrow, Alaska (1972–2010) *Environ. Res. Lett.* **7** 015508
Walker D *et al* 2012 Environment, vegetation and greenness (NDVI) along the North America and Eurasia Arctic transects *Environ. Res. Lett.* **7** 015504

Walvoord M A, Voss C I, Ebel B A and Minsley B J 2019 Development of perennial thaw zones in boreal hillslopes enhances potential mobilization of permafrost carbon *Environ. Res. Lett.* **14** 015003

Walvoord M A, Voss C I and Wellman T P 2012 Influence of permafrost distribution on groundwater flow in the context of climate-driven permafrost thaw: example from Yukon Flats Basin, Alaska, United States *Water Resour. Res.* **48** W07524

Woo M-K, Kane D L, Carey S K and Yang D 2008 Progress in permafrost hydrology in the new millennium *Permafr. Periglac. Process.* **19** 237–54

Xue K *et al* 2016 Tundra soil carbon is vulnerable to rapid microbial decomposition under climate warming *Nat. Clim. Change* **6** 595–600

Zhang K, Kimball J S M Q, Jones L A, Goetz S J and Running S W 2009 Satellite based analysis of northern ET trends and associated changes in the regional water balance from 1983 to 2005 *J. Hydrol.* **379** 92–110

Zhang K, Kimball J S, Hogg E H, Zhao M, Oechel W C, Cassano J J and Running S W 2008 Satellite-based model detection of recent climate-driven changes in northern high-latitude vegetation productivity *J. Geophys. Res.* **113** G03033